Structure, magnetic and microwave studies of mechanically alloyed powders Fe45Ni35Co20

Ahmed Haddad[1] ✉, *Insaf Ouldbrahim*[1], *Mohamed Azzaz*[2]

[1]*Ministry of Higher Education and Scientific Research, Research Center in Industrial Technologies CRTI, P.O. Box 64, Cheraga 16014, Algiers, Algeria*
[2]*Laboratoire des Sciences et Génie des Matériaux, Faculty of Mechanical Engineering and Process Engineering, University of Sciences and Technologie Houari Boumediene, Algeria, Algeria*
✉ *E-mail: haddad_ah@hotmail.com*

Published in Micro & Nano Letters; Received on 11th September 2017; Revised on 20th March 2018; Accepted on 27th March 2018

Nanocrystalline Fe-35 wt%Ni-20 wt%Co has been prepared by using a high-energy planetary ball mill with increasing milling time from 4 to 36 h. Microstructural characterisations showed the development of an face-centred cubic nanostructured Fe-35 wt%Ni-20 wt%Co alloy with an average crystallite size of 8 nm. The magnetic investigation revealed that the nanostructures obtained from a milling time of 36 h have the highest magnetic saturation and the lowest coercive field. In addition, the hardness and the electromagnetic absorption of the Fe-35 wt%Ni-20 wt%Co alloy were found to increase with the milling time. These evolutions could be attributed to the crystallite size and the strain variations in the samples during milling.

1. Introduction: Nanocrystalline materials, iron-based alloys have received remarkable attention due to their excellent soft magnetic properties such as high saturation magnetisation (MS), high permeability and good absorption properties. These characteristics result from the refinement of the crystallite size up to the nanoscale and the large fraction of the atoms residing in the grain boundaries. They are very sensitive to the microstructure of the alloy formation and the effects of elementary additions on the microstructures [1]. There are different methods for producing iron-based magnetic alloys. Mechanical alloying (MA) is one among these methods which is a simple method of processing to produce a large variety and large quantities of nanomaterials at the solid state [2]. The nickel–iron (Ni–Fe) alloys possess the highest permeability and exhibit the least amount of flux density. It is known that Fe–Ni alloys are kinds of important soft magnetic materials, which have wide application in the field of electronic devices and industry. Fe–cobalt (Co) alloys soft magnetic materials have the highest saturation MS, as well as high Curie temperatures, making these alloys suitable materials for high-temperature application [3]. Properties vary over composition range; optimum composition must be selected for a particular application.

The soft magnetic property of Fe–Ni alloys change with Ni%: lower coercive field (about 80 wt% Ni), and higher MS (about 50 wt% Ni) and the Fe–Co magnetic alloys with compositions of 25–50 wt% Co have the highest moment per unit mass and the maximum (*Ms*) occurs at 35 wt% Co, and of 65 wt% the smallest coefficient of reflection and maximum absorption [4, 5].

Furthermore, Co–Fe–Ni ternary alloys exhibit good soft magnetic properties that suggest several applications, for instance, write head core materials in hard-disk drives [6, 7]. However, there are only a few works available on the detailed investigation of the effect of substitution elements on the evolution of nanocrystalline microstructure and the resulting magnetic properties of FeCoNi alloy powders with %Co more than %Ni≤20% of Fe [7, 8].

In the present Letter, we have further clarified the effect of MA on both microstructure and magnetic properties of the Fe-35 wt% Ni-20wt%Co the system at various milling times. The concentrations ∼of 50 wt% Co and ∼of 80 wt% Ni which have not reserved much investigation in the literature.

2. Experimental details: The present Letter carries out the structure study and magnetic properties of MA (45 wt% Fe-35wt% Ni-20wt%Co) powders. Elemental powders with high purity (Fe (∼50 µm, 99.9%), Ni (∼5 µm, 99.98%) and Co (∼30 µm, 99.9%) have been used as starting materials and mixed at the desired composition. The milling process was performed under inert atmosphere (high purity argon 99.9% purity) using a planetary high-energy ball mill. The weight ratio between the balls and the powders was maintained at 20:1. The milling powder ball was carried out using a sequence of 30 min milling and 15 min resting. The milling time sequence was chosen to avoid contamination from the friction and the impacts between the balls and the walls of the vials. The milling times were 4, 8, 12, 18 and 36 h. To avoid oxidation, powders were introduced under argon atmosphere, into a cylindrical steel container (vial) with 40 steel balls (Ø, 20 mm; mass, 32 g) and 250 rpm rotation speed.

To check crystal structure and to determine the effective grain size, we used X-ray diffraction (XRD) measurements (Siemens D500 diffract meter) using Cu Kα radiation ($\lambda = 1.5406$ Å) in the 2θ range from 30° to 110°. For each milling times, three measurements were done. The crystallite size and lattice strain were estimated by Williamson–Hall method, and the phase identification was determined by using HighScore Plus software (Version 3.0d).

Morphology and particle size were observed via scanning electron microscopy (SEM) model (XL 30S FEG) coupled with energy dispersive X-ray spectroscopy. The average magnetic properties were measured at room temperature using a MICROSENS EV9 Vibrating Sample Magnetometer. To further understand the alloying mechanism during MA, available powders were mixed with a resins epoxy to get bulk samples, and then prepared for microhardness tests by polishing.

According to the transmission line theory, the reflection loss (RL) of electromagnetic radiation Re (dB) which has been measured using a metallic waveguide (PM 7001X) in the X-band frequency at 9.5 GHz, under normal incidence of the electromagnetic field.

3. Results and discussion

3.1. Structure: The evolution of XRD patterns with milling time is shown in Fig. 1*a*, where the diffraction of the powders Fe45Ni35Co20 showed the presence of [body-centred cubic (BCC)] Fe, hexagonal close-packed and face-centred cubic (FCC) cobalt and nickel. Co and Ni peaks disappeared after 4 and 8 h of

doi: 10.1049/mnl.2017.0655

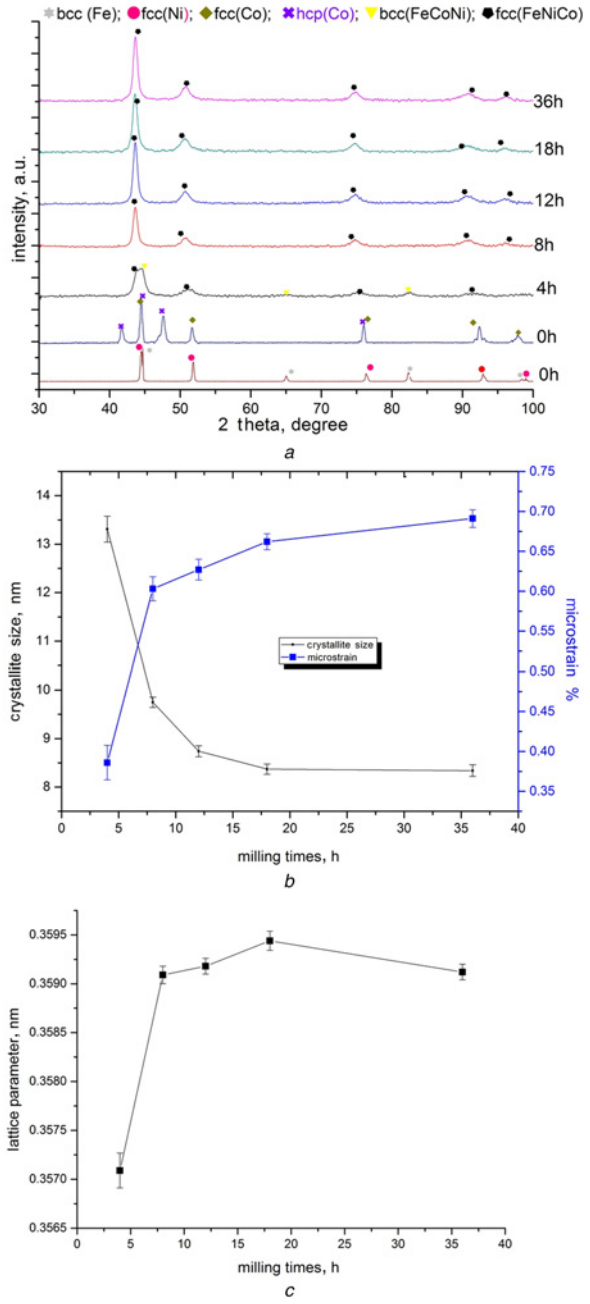

Fig. 1 *Evolution of XRD patterns with milling time*
a X-ray patterns for various milling times
b Evolution of average crystallite size and lattice parameter
c Microstrain during MA

milling, respectively, indicating the formation of new phase BCC Fe(Co–Ni) and FCC Fe(Ni–Co) solid solution due to the penetration of Co and Ni atoms into Fe lattice. The energy and the time of milling have a complex effect on the final structure of the alloy. The increase in milling energy has impact through two main physical parameters: the different types of structure defect and the milling process average temperature. Dissolution sequence (DS) of elements during MA depends on several factors including intrinsic properties of elements (such as melting points, bonding energies and mechanical properties) and solute content.

Therefore, based on the melting point, the DS can be determined as Ni→Co→Fe [4, 6]. A possible explanation for the reverse tendency between Co and Ni was proposed with mechanical disintegration and solute content, the amount of Ni was about 1.75 times the Co content in this system associated with the progressive mutual dissolution of the elemental Co and Ni powders giving rise to the formation of two FCC solid solution Ni(Co) and Co(Ni). Indeed, it is well established that the diffusivity of Co into Ni is larger than that of Ni in Co [9, 10]. Moreover, an increase of the milling temperature (energy of milling) will stabilise and destabilise FCC and BCC structures, respectively, as mentioned according to the Fe–Ni phase diagram [11]. An increase of the milling intensity will extend the FCC concentration range and narrow the BCC concentration range (Fig. 1*a*). The structure defects caused by the MA, lead to a lesser destabilisation of the FCC phase than of the BCC phase [9]. The evolution of crystallite size and lattice strain as a function of milling time is shown in Fig. 1*b*. The average crystallite size decreased rapidly up to 12 h of milling due to the formation of solid solution and then attained a saturated value. In fact, when the grain size reaches a saturation value, further milling will not produce more dislocations due to the difficulty of generating dislocations at small grain sizes, though existing dislocations will be rearranged and some will be annihilated [12]. Also, we have noted that the lattice parameter increases with increasing milling time, which is due to the heavily cold worked and plastically deformed powders and by defects introduced in interfaces. At the same time, we observe both a considerable decrease in the grain size and increase in the volume fraction of grain boundaries. The grain-boundary affects the movement of dislocation and strain hardening significantly. On the basis of the coherent polycrystalline model [7], the volume fraction of the grain boundaries f_{gb} was estimated by the formula

$$f_{gb} = 1 - f_g \tag{1}$$

where f_g denotes the volume fraction of the grains given by

$$f_g = \frac{(D-d)^3}{D^3} \tag{2}$$

Moreover, D is the crystallite size, d is the effective grain-boundary thickness. In most of the nanostructured alloys, the estimated thickness of the interfaces was roughly found at 2–3 atomic layers [5, 7].

The elemental analysis data are shown in Fig. 2 showed that the Fe–Co ratios evaluated for 4 h (1.91) and 36 h (2.53) milling times are very close to the starting nominal composition 2.25. One concludes that the contamination by the constituents (Cr) of the steel from both vials and balls can be neglected and the absence of oxygen indicates the non-oxidation of elements.

3.2. Morphology: The evolution of particle's morphology as a function of milling time is shown in Fig. 3. We observed that different morphologies are presented during the MA stages.

Microstructure formation during MA is administrated by a competition between the cold welding and a fracture of powder particles under the repetitive events of impact [13].

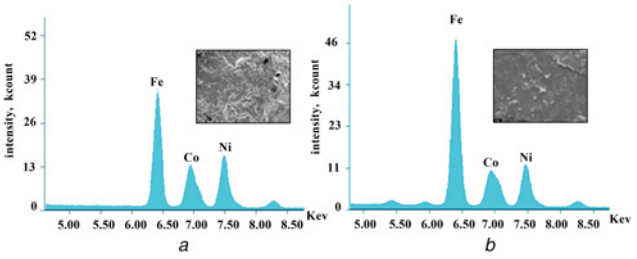

Fig. 2 *Quantitative analysis spectra of the Fe45Ni35Co20*
a 4 h milling
b 36 h milling

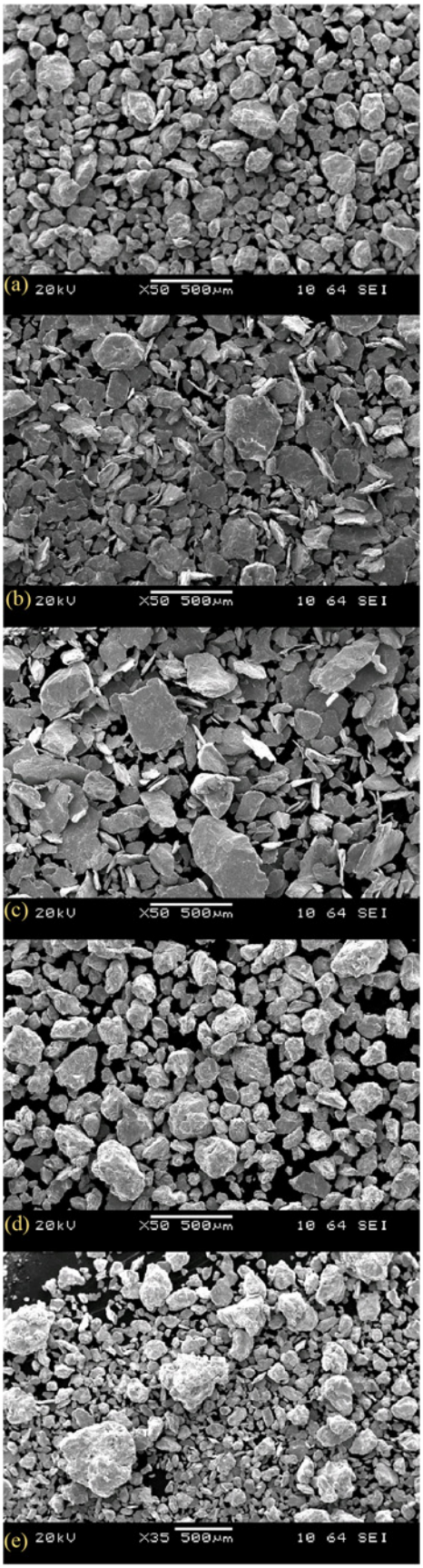

Fig. 3 *Morphology of Fe45Ni35Co20 alloy*
a 4 h of milling time
b 8 h of milling time
c 12 h of milling time
d 18 h of milling time
e 36 h of milling time

It is well known that during the milling of ductile–ductile systems, the powders become flattened, cold welded, fracture and rewelded. In the early stages of milling of ductile materials, the morphology changes significantly after few hours of milling (8 h, Fig. 3*b*) the powders are crushed and changed into flake shape with different sizes (these different sizes of particles are commonly seen in early stages). The powder particles are flattened by the energy induced by the contacts between (ball–powder–ball) and/or (ball–powder–bottle). This leads to the changing of morphology and an increase in particle size (though some small particles are produced). For the milling time at 12 h, the mean particle size increased because the propensity of cold welding dominates the milling process. At this stage, the powders tend to turn to an irregular shape and size (Fig. 3*b*), a large distribution of particles sizes is observed. With continued deformation up to 18 h (Fig. 3*c*), fracturing becomes dominant because the particles get work harder and fracture by a fatigue failure mechanism [14, 15]. Therefore, in Fig. 3*d*, the particle shape becomes more regular, spherical and smaller particle size is observed, this can be attributed to the balance between the fracturing and the welding processes. However, the formation of an irregular distribution of particle sizes at 36 h of milling (Fig. 3*e*) reveals that the step of balance between the fracturing and the welding processes is exceeded.

The mechanical behaviour of the alloy was studied by measuring the microhardness Vickers 'Hv' at the room (Fig. 4). No microcracking was observed from the corners or sides of the Vickers indentation, indicating a rather high fracture resistance of the material. When the dissolved atoms are dissolved in the solid solution, this tends to increase the hardness (the powder becomes more regular) [16]. The accumulation of strain energy during MA (by increasing milling times) tends to increase the microhardness value [3, 17]. The behaviour of the dislocation is inversely related to the macroscopic grain size. The grains in severely deformed materials are divided into sub-grains or dislocation cells, which are separated from each other by grain boundaries. As the deformation continues, these dislocation walls finally transform into grain boundaries. The grain-boundary affects the movement of dislocation and strain hardening significantly, as well as, the strength and ductility of materials.

Magnetic properties (were measured at room temperature) might be affected by changes as well as in the structure as in the milling times, particularly coercivity field (*Hc*), and the saturation *Ms* which remain important parameters [12]. *Hc* is often affected by grain size and most types of structural defects, precipitates, dislocations, grain boundaries and non-magnetic particle distribution. Additionally, in the mechanical alloy, the evolution of *Hc* is

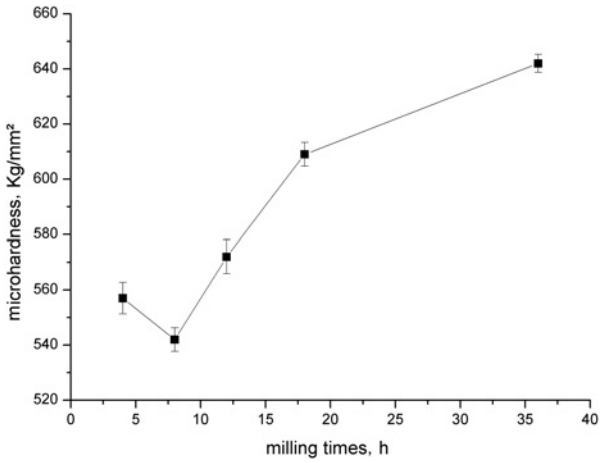

Fig. 4 *Average microhardness as a function of milling times*

doi: 10.1049/mnl.2017.0655

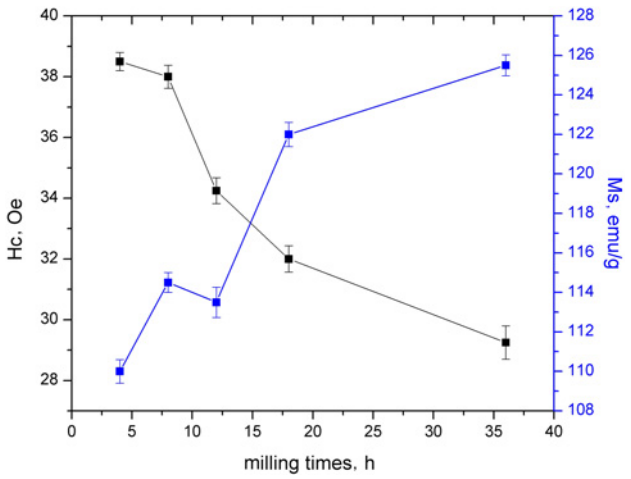

Fig. 5 *Evolution of average Ms and Hc functions of milling time*

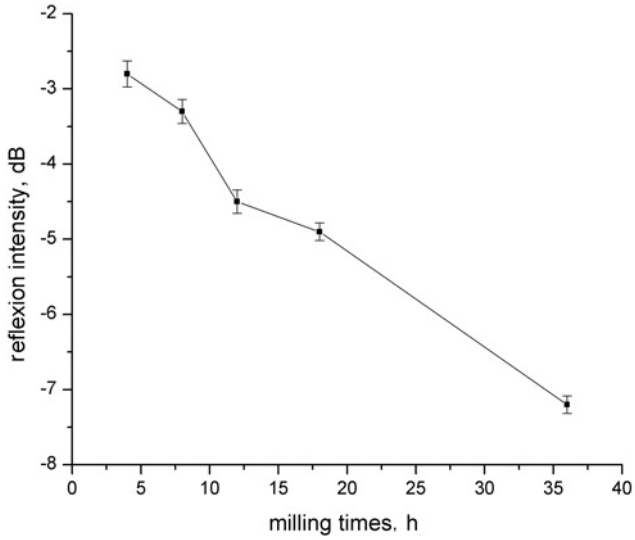

Fig. 6 *RLs according to the milling times*

due to the internal nanostructure, impurities, pores and defects that are introduced during milling. The maximum *Hc* is obtained at 4 h milling with the presence of BCC FeCoNi, after that the *Hc* decreases down, suggests the formation of FCC FeNiCo (Fig. 5).

The important reduction of the crystallites size and each grain behaves as a magnetic domain (mono-domain grain) thus reduce the influence of block's partitions, which leads to an easier rotation of the domain walls than the *Ms* increase when milling time is increased. In fact, this leads to the reduction in magnetocrystalline anisotropy and also charge transferring between the ferromagnetic atoms [18, 19].

The microwave properties of the alloy depend on both characteristics of the particles and their microstructures such as particle size, powder morphology, texture, saturation MS and magnetic anisotropy field [8]. The variations of the RLs according to the milling times at 9.5 GHz are represented in Fig. 6. This evolution of RL is due to the presence of defects generated during intensive milling and the volume fraction of the grain boundaries [13]; these parameters create multiple reflections and interfacial polarisations making possible to improve the absorbing property of microwaves and evolution of the thickness when the volume fraction changes. It is clear enough that the FeNiCo alloy becomes more absorbing with milling time increasing.

4. Conclusion: A nanostructured Fe45Ni35Co20 alloy was obtained by MA. The evolution of microstructure and magnetic properties of the powders during milling was investigated using XRD, SEM and vibrating sample magnetometer. The morphologies of the powder at different milling times are governed by the fracturing and welding processes. The formation of platelet particles due to the dominance of cold welding and second the fracturing process leads to spherical particles. In addition, the shape of the particle becomes more regular and spherically smaller when the balance between fracturing and welding processes is reached. During the milling for 4 h leads to the formation of two BCC and FCC, the predominate phases (FeCoNi and FeNiCo) coexist, as milling times increasing the phase FCC (FeNiCo) became the covering of solid solution. On the basis of XRD evolution, DS was determined as Co→Ni→Fe. The increase of the microhardness value is mainly attributed to the accumulation of strain energy and relation to the higher-volume fraction of grain boundaries. The evaluation of coercive field *Hc*, RLs and crystallite size reveals that there is a regular and a similar diminution. On the other hand, the MS increases when the milling time is increased.

5 References

[1] Neamţu B.V., Chicinaş H.F., Ababei G., *ET AL.*: 'A comparative study of the Fe-based amorphous alloy prepared by mechanical alloying and rapid quenching', *J. Alloys Compd.*, 2017, **703**, (Supplement C), pp. 19–25

[2] Loginov P.A., Levashov E.A., Kurbatkina V.V., *ET AL.*: 'Evolution of the microstructure of Cu–Fe–Co–Ni powder mixtures upon mechanical alloying', *Powder Technol.*, 2015, **276**, (Supplement C), pp. 166–174

[3] Haddad A., Zergoug M., Azzaz M., *ET AL.*: 'Monitoring of metal powder by eddy current', *Int. J. Microstruct. Mater. Prop.*, 2010, **5**, (1), pp. 3–14

[4] Yousefi M., Sharafi S.: 'The effect of simultaneous addition of Si and Co on microstructure and magnetic properties of nanostructured iron prepared by mechanical alloying', *Mater. Des.*, 2012, **37**, pp. 325–333

[5] Chen Y.-L., Hu Y.-H., Hsieh C.-A., *ET AL.*: 'Competition between elements during mechanical alloying in an octonary multi-principal-element alloy system', *J. Alloys Compd.*, 2009, **481**, (1-2), pp. 768–775

[6] Yousefi M., Rahmani K., Amiri Kerahroodi M.S.: 'Comparison of microstructure and magnetic properties of 3% Si-steel, amorphous and nanostructure finemet', *J. Magn. Magn. Mater.*, 2016, **420**, (Supplement C), pp. 204–209

[7] Raanaei H., Eskandari H., Mohammad-Hosseini V.: 'Structural and magnetic properties of nanocrystalline Fe–Co–Ni alloy processed by mechanical alloying', *J. Magn. Magn. Mater.*, 2016, **398**, pp. 190–195

[8] Yuping D., Yahong Z., Tongmin W., *ET AL.*: 'Evolution study of microstructure and electromagnetic behaviors of Fe–Co–Ni alloy with mechanical alloying', *Mater. Sci. Eng. B*, 2014, **185**, pp. 86–93

[9] Loudjani N., Bensebaa N., Dekhil L., *ET AL.*: 'Structural and magnetic properties of Co50ni50 powder mixtures', *J. Magn. Magn. Mater.*, 2011, **323**, (23), pp. 3063–3070

[10] Jiraskova Y., Bursik J., Turek I., *ET AL.*: 'Phase and magnetic studies of the high-energy alloyed Ni–Fe', *J. Alloys Compd.*, 2014, **594**, pp. 133–140

[11] Valderruten J.F., Pèrez Alcazar G.A., Greneche J.M.: 'Study of Fe–Ni alloys produced by mechanical alloying', *Phys. B, Condens. Matter*, 2006, **384**, (1-2), pp. 316–318

[12] Yousefi M., Sharafi S., Mehrolhosseiny A.: 'Correlation between structural parameters and magnetic properties of ball milled nanocrystalline Fe–Co–Si powders', *Adv. Powder Technol.*, 2014, **25**, (2), pp. 752–760

[13] Jun L.I.U., Yongbao F., Tai Q.I.U.: 'Synthesis, characterization, and microwave absorption properties of Fe-40 Wt%Ni alloy prepared by

mechanical alloying and annealing', *J. Magn. Magn. Mater.*, 2011, **323**, (23), pp. 3071–3076
[14] Glezer A.M., Tomchuk A.A., Sundeev R.V., *ET AL.*: 'Two-phase' model of the structure formed upon severe plastic deformation in A-Fe and feni alloy', *Mater. Lett.*, 2015, **161**, pp. 360–364
[15] Krasnowski M.: 'Phase transformations during mechanical alloying and subsequent heating of FeAlB powders', *J. Alloys Compd.*, 2017, **706**, (Supplement C), pp. 110–115
[16] Greneche J.M., Ślawska-Waniewska A.: 'About the interfacial zone in nanocrystalline alloys', *J. Magn. Magn. Mater.*, 2000, **215-216**, (Supplement C), pp. 264–267
[17] Zhang Q., Xu H., Tan X.H., *ET AL.*: 'The effects of phase constitution on magnetic and mechanical properties of feconi(cual)X (X = 0–1.2) high-entropy alloys', *J. Alloys Compd.*, 2017, **693**, (Supplement C), pp. 1061–1067
[18] Yu P.F., Zhang L.J., Cheng H., *ET AL.*: 'The high-entropy alloys with high hardness and soft magnetic property prepared by mechanical alloying and high-pressure sintering', *Intermetallics*, 2016, **70**, (Supplement C), pp. 82–87
[19] Karimi L., Shokrollahi H.: 'Structural, microstructural and magnetic properties of amorphous/nanocrystalline Ni63fe13mo4nb20 powders prepared by mechanical alloying', *J. Alloys Compd.*, 2011, **509**, (23), pp. 6571–6577

doi: 10.1049/mnl.2017.0655